Neuroscience

The Na^+ leak channel NALCN controls spontaneous activity and mediates synaptic modulation by α2-adrenergic receptors in auditory neurons

Tenzin Ngodup, Tomohiko Irie, Sean Elkins, Laurence O. Trussell

Oregon Hearing Research Center and Vollum Institute, Oregon Health & Science University, Portland OR USA • Department of Physiology, Kitasato University School of Medicine, Sagamihara, Japan

Reviewed Preprint

Revised by authors after peer review.

About eLife's process

Reviewed preprint version 2
December 18, 2023 (this version)

Reviewed preprint version 1
July 25, 2023

Posted to bioRxiv
June 25, 2023

Sent for peer review
June 6, 2023

Abstract

Cartwheel interneurons of the dorsal cochlear nucleus (DCN) potently suppress multisensory signals that converge with primary auditory afferent input, and thus regulate auditory processing. Noradrenergic fibers from locus coeruleus project to the DCN, and α2-adrenergic receptors inhibit spontaneous spike activity but simultaneously enhance synaptic strength in cartwheel cells, a dual effect leading to enhanced signal- to-noise for inhibition. However, the ionic mechanism of this striking modulation is unknown. We generated a glycinergic neuron-specific knockout of the Na^+ leak channel NALCN, and found that its presence was required for spontaneous firing in cartwheel cells. Activation of α2-adrenergic receptors inhibited both NALCN and spike generation, and this modulation was absent in the NALCN knockout. Moreover, α2-dependent enhancement of synaptic strength was also absent in the knockout. $GABA_B$ receptors mediated inhibition through NALCN as well, acting on the same population of channels as α2 receptors, suggesting close apposition of both receptor subtypes with NALCN. Thus, multiple neuromodulatory systems determine the impact of synaptic inhibition by suppressing the excitatory leak channel, NALCN.

eLife assessment

This paper reports the **fundamental** discovery of adrenergic modulation of spontaneous firing through the inhibition of the Na+ leak channel NALCN in cartwheel cells in the dorsal cochlear nucleus. This study provides unequivocal evidence that the activation of alpha-2 adrenergic or GABA-B receptors inhibit NALCN currents to reduce neuronal excitability. The evidence supporting the conclusions is **exceptional**, the electrophysiological data is high quality and the experimental design is rigorous.

Introduction

The dorsal division of the mammalian cochlear nucleus (DCN) is a cerebellum-like structure in which principal cells integrate multimodal activity with primary auditory afferents, and these converging signals are thought to contribute to sound localization and sensitivity to sounds of interest (May, 2000; Oertel and Young, 2004). Cartwheel cells (CWC) are cerebellar Purkinje cell homologs that potently control this convergence by gating the multimodal signals to postsynaptic fusiform principal cells. CWCs also receive inputs from various neuromodulatory systems, including noradrenaline (NA) (Trussell, 2019). We showed previously that agonists of α2 noradrenergic receptors simultaneously halts spontaneous spike activity and enhances the strength of inhibitory signals to fusiform cells (Kuo and Trussell, 2011). The mechanism for this paradoxical action depends on the effect of spontaneous activity on synaptic strength: by reducing ongoing presynaptic firing, recovery from synaptic depression ensues and allows CWCs to mediate stronger postsynaptic signals in the fusiform cells. A related mechanism was later identified in the action of oxytocin in hippocampal interneurons (Owen et al., 2013; Tirko et al., 2018). However, the mechanism by which α2 noradrenergic receptors controlled such activity remained obscure. The most obvious candidate ion channel that could mediate such inhibition is the GIRK channel (G -protein-gated inwardly rectifying K^+ channel) (Luscher et al., 1997; Arima et al., 1998; Li and van den Pol, 2005; Philippart and Khaliq, 2018), however attempts in our laboratory to implicate this channel failed.

The Na^+ leak channel NALCN functions as a complex of 4 proteins: NALCN, FAM151a, UNC79 and UNC80 (Lu et al., 2010; Ren, 2011; Cochet-Bissuel et al., 2014; Kschonsak et al., 2020; Xie et al., 2020). This channel complex (here termed simply NALCN) contributes to the depolarizing drive for spontaneous firing in a wide variety of neurons, and functions in sensory, motor and circadian pathways (Nash et al., 2002; Lu et al., 2007; Lu and Feng, 2011; Xie et al., 2013; Lutas et al., 2016; Shi et al., 2016). Accordingly, mutations in the NALCN subunit or its associated proteins are linked to a variety of human diseases (Al-Sayed et al., 2013; Cochet-Bissuel et al., 2014; Chong et al., 2015; Bramswig et al., 2018). A hallmark of this channel is its inhibition by extracellular Ca^{2+}; reduction of extracellular Ca^{2+} enhances the current, permitting a ready assessment of NALCN's presence in neurons (Lu et al., 2010; Ren, 2011; Philippart and Khaliq, 2018; Chua et al., 2020). Recently it was shown that neurons of the substantia nigra express NALCN, and that both dopamine and $GABA_B$ receptors strongly downregulated NALCN activity in this region (Lutas et al., 2016; Philippart and Khaliq, 2018). As global knockouts of NALCN die at birth (Lu et al., 2007), we generated a knockout mouse line specific to glycinergic neurons in order to test the role of this channel in auditory interneurons. We found that CWCs expressed functional NALCN, and its loss in NALCN knockouts led to cessation of spontaneous firing. Outward currents and inhibition of firing mediated by NA was eliminated in the knockouts; since NALCN generates inward excitatory currents, NA must act by inhibition of NALCN. Similar results were obtained for the $GABA_B$ agonist baclofen. Thus, NALCN serves multiple roles in auditory function, setting the pace of neuronal firing while also mediating electrical inhibition by multiple neuromodulators and enhancement of synaptic strength.

Results

NALCN and modulation of spike generation

In order to assess the role of NALCN in modulation of spontaneous firing of CWCs, we generated an NALCN knockout mouse by crossing a floxed NALCN mouse line B6(Cg)-*Nalcn*$^{tm1c(KOMP)Wtsi}$/DrenJ with a GlyT2-cre line, thus deleting NALCN from glycinergic neurons (Methods). NALCN$^{-/-}$ mice were slightly smaller than wildtype mice (weight ratio, 4:3) but had normal hearing, as assessed by auditory brainstem responses (**Figure 1-figure supplemental**

1), and the morphology of their CWCs was characteristic of those of wildtype mice (**Figure 1-figure supplemental 2**; (Bender and Trussell, 2009)). 'Wildtype' mice used here were either C57/BL6 or GlyT2-EGFP (Zeilhofer et al., 2005; Kuo et al., 2012; Ngodup et al., 2020) in which GFP is expressed in glycinergic neurons. CWC were recorded using cell-attached mode to monitor baseline spontaneous firing and the inhibition of firing by NA. Except as noted below, all recordings were made in physiological Ca^{2+} concentration (1.2 mM). In confirmation of previous studies in wildtype mice (Kim and Trussell, 2007; Kuo and Trussell, 2011) 71% of CWC exhibited spontaneous firing (mean firing rate, 17.74 ± 2.31 Hz) and bath application of 10 μM NA completely and reversibly eliminated such firing in every case (N = 8, **Fig. 1A & B**). However, in experiments on NALCN KO mice, CWC showed no spontaneous firing (**Fig 1C & D**; N = 6; difference from wildtype type, $p < 0.0005$), and thus NA had no additional effects on spontaneous firing (mean firing rate, KO = 0 ± 0 Hz, NA = 0; N = 6). Thus, NALCN likely provides a tonic inward current necessary to drive spontaneous firing in CWC. These effects were not accompanied by changes in membrane input resistance (WT: 135.34±21.53 MΩ (n=18) vs KO: 132.19±16.11 MΩ (n=15), p=0.46, t-test).

Although NALCN supports spontaneous firing, it was not clear whether the effect of NA is mediated through NALCN or some other channel. To explore this problem, we first examined evoked firing in CWC and the effects of NALCN and NA. CWC were recorded in current-clamp mode, and a family of negative and positive, 600-ms current pulses were delivered in 25-pA steps (**Fig 2A1**). In response to positive pulses, CWCs fire mixtures of simple (single) spikes and complex spikes, the latter containing Na^+ spike clusters driven by a Ca^{2+}-dependent current (Kim and Trussell, 2007). The timing of spikes during each current pulse was used to generate raster plots of firing (**Fig 2A2**), and the number of spikes at each current step was used to plot a frequency vs current intensity curve (**Fig 2E**). In the same set of cells, we then applied NA and repeated the current steps (**Fig 2B & E**). NA hyperpolarized the resting potential by −1.90 ± 0.24 mV and increased the current level required to initiate firing (rheobase, **Fig 2E**), indicating that NA reduced excitability. However, we also observed a suppression of the peak firing rate in NA; similar rundown of peak firing rate could be observed without change in rheobase as a result of whole-cell recording over this time period (see also Kim and Trussell, 2007), and thus frequency-intensity plots were normalized to peak intensity (**Fig 2F**). This manipulation revealed a clear shift to the right in the onset of firing (i.e., toward higher intensity) as a result of NA. Rheobase was defined as the current intensity at which spiking was 20% of maximum. Using this criterion, NA generated a significant increase in rheobase in response to current pulses (Ctrl, rheobase = 91.40 ± 11.35 pA, NA, 168.59 ± 14.89 pA, $p = 0.0011$ (t-test)). Control experiments established that wash-in of NA with the α2 blocker idazoxan did not lead to a change in rheobase (Ctrl, rheobase = 95.11 ± 16.86 pA, NA + idazoxan, 105.88 ± 21.89 pA, N = 9, $p = 0.38$ (t-test)), showing that the shift in rheobase was a genuine effect of α2 receptors (**Fig 2I, J**). This protocol was then applied to NALCN KO mice (**Fig 2C, D, G & H**). Although CWCs showed no spontaneous firing, they were able to respond to current steps with mixtures of simple and complex spikes, and peak firing rates did not differ from wildtypes (rheobase, Ctrl, 91.40 ± 11.35 pA; KO, 120.81 ± 17.53 mV, N = 11, $p = 0.08$ (t-test)). However, unlike wildtype mice, the NALCN KO mice showed no significant shift in rheobase with NA (KO, rheobase = 120.81 ± 17.53 pA, NA, 158.0 ± 12.16 pA, n = 11, $p = 0.064$ (t-test) (**Fig 2H**).

In order to test whether the effects of NA on rheobase and evoked spiking is primarily due to the small hyperpolarization induced by NA, we mimicked this effect of NA by injecting current to CWC to hyperpolarize the membrane by the same amount as induced by NA (approximately 2 mV), and then repeated the current injection protocol (**Figure 2-figure supplement 1**). Under these conditions, we were able to replicate the effects of NA on CWC rheobase and evoked firing (rheobase Ctrl = 70.88 ± 7.68 pA, hyperpolarized = 125 ± 12.90 pA, N = 6, $p = 0.0009$). We then compared the ratio of the changes in rheobase in NA with respect to control under different conditions, also comparing to the relative effects of current injection. These comparisons confirmed that NA shifts rheobase dependent upon NALCN, and that this effect is likely caused by

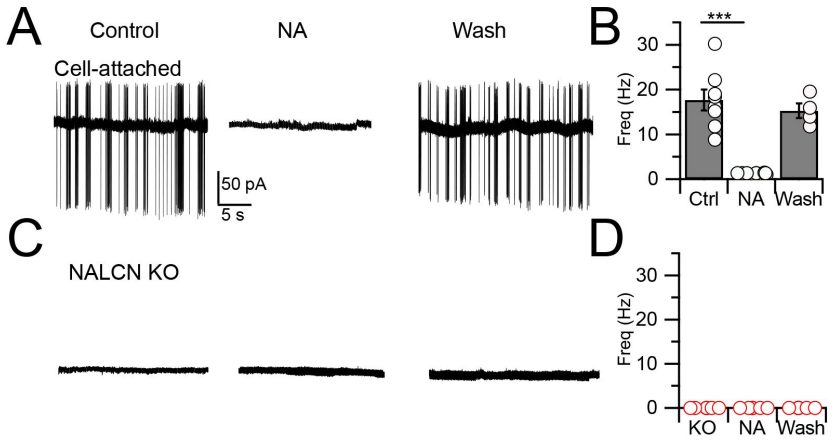

Figure 1

Spontaneous firing is absent in NALCN KO mice. A, Representative cell-attached recording from a spontaneously spiking CWC in control. NA (10 μM) applied to the bath in the middle trace, and washout on the right-most trace. B, Spontaneous spike rate in control, NA and washout, showing that NA eliminated spontaneous spiking in CWCs (n=6 cells). C, Representative trace showing absence of spontaneous firing in a CWC from a NALCN KO mouse. NA had no effect on firing. D, Summary of spontaneous firing and lack of NA effect in CWC from NALCN KO mice (n = 5 cells).

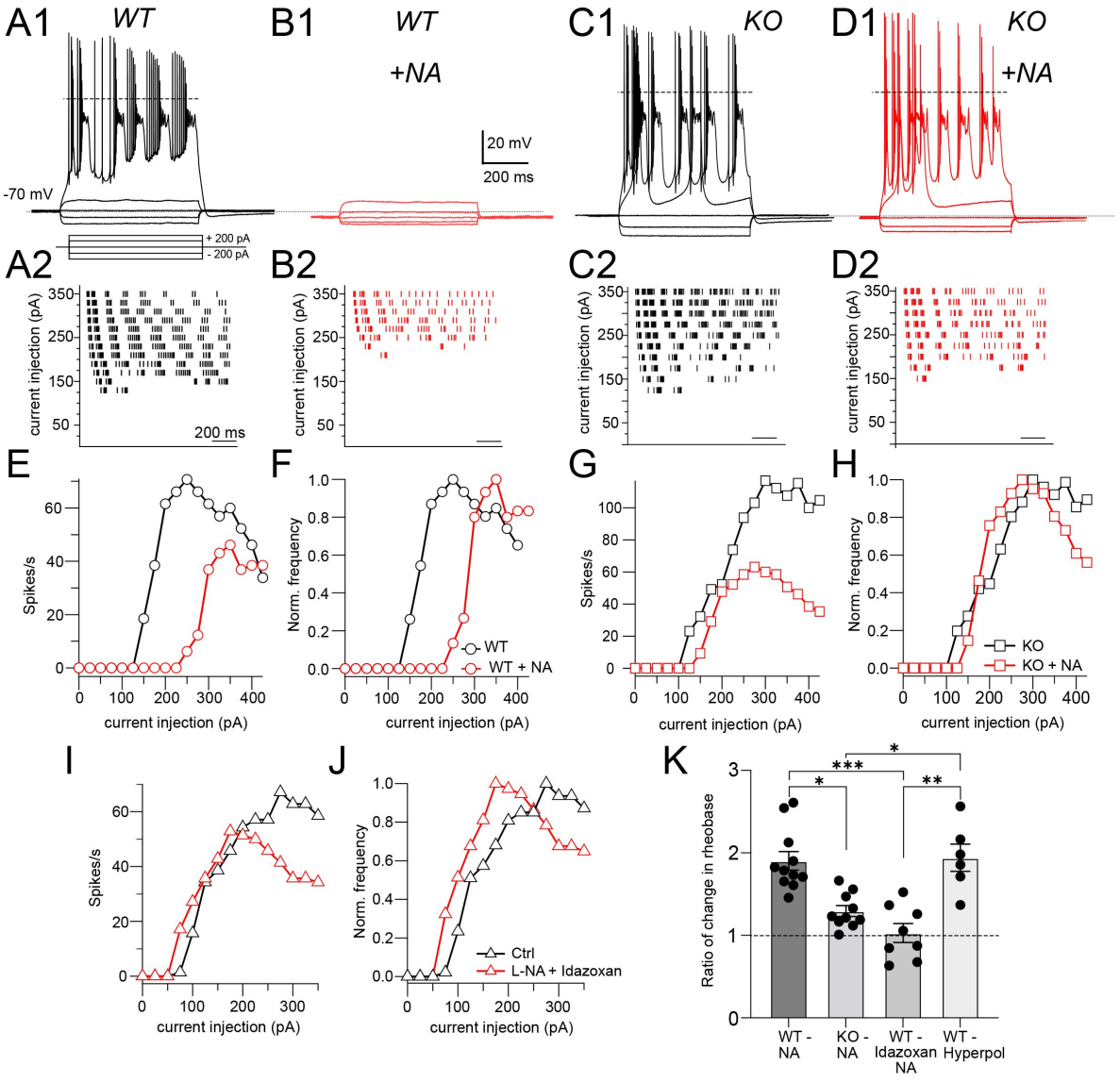

Figure 2

NALCN is required for NA-mediated shift in rheobase. A1, Profile of voltage responses to current steps. Simple and complex spikes evoked by +200 pA. A2, Raster plot of spike timings during different level of current injection. B1, B2, same cell as in A but in presence of 10 µM NA (indicated by red traces and markers). C, D as in A, B but for recordings from a CWC from a NALCN KO mouse. E, Spike rate calculated from data in A2 and B2 plotted as function of current level. F, Data from E normalized to peak firing rate. G, Spike rate calculated from data in C2 and D2 plotted as function of current level. H, Data from G normalized to peak firing rate. I, Summary data (mean ± SEM) for ratio of change in rheobase of CWC from WT and KO mice with 10 µM NA, NA + idazoxan, and hyperpolarization conditions. Significance: * <0.05; ** < 0.01; *** < 0.001. Dashed line in A1, C1, D1 indicates zero mV.

membrane potential hyperpolarization (**Fig. 2K**: Ctrl = 1.90 ± 0.11, KO = 1.25 ± 0.05, Idazoxan = 1.03 ± 0.11, hyperpolarized = 1.94 ± 0.16, $p < 0.0001$, non-parametric Kruskal-Wallis; post hoc Dunn's test, Ctrl vs KO $p = 0.0086$, Ctrl vs idazoxan $p = 0.0007$, KO vs hyperpolarized $p = 0.02$, idazoxan vs hyperpolarized $p = 0.0028$).

Outward response generated by suppression of NALCN

As cessation of spontaneous activity and elevation of rheobase by NA is likely associated with an outward, inhibitory current, we performed voltage-clamp experiments to determine the magnitude of that current in wildtype and KO mice, and its pharmacological sensitivity. Using a patch-pipette fill containing high K^+ (Methods), cells were held at −65 mV and a 5-ms puff of NA was applied near the soma using a pressure-ejection pipette. Under these conditions, a slowly rising outward current was observed that decayed over a time course of 10-15 seconds (**Fig 3A**). As G-protein coupled inward rectifier channels (GIRK) are known to mediate α2 receptor effects in some brain regions (Williams et al., 1985; Aghajanian and Wang, 1986; Arima et al., 1998; Li and van den Pol, 2005; Nimitvilai et al., 2017), we tested the role of GIRK channels using the GIRK blocker Ba^{2+}. However, $BaCl_2$ (100 μM) had no significant effect on the amplitude of the NA-evoked current (**Fig 3A, C**) (Ctrl = 15.44 ± 1.66 pA; $BaCl_2$ = 12.86 ± 1.44, N = 6, $p = 0.133$). When this experiment was repeated in NALCN KO mice, the NA-evoked current was only 12.5% of that observed in wildtype mice (**Fig 3B & C**). Although the amplitude of the NA-evoked current in the knockout was only a few pA, bath application of $BaCl_2$ nevertheless produced a statistically significant block of this small residual current, essentially eliminating all response to NA (KO = 1.93 ± 0.83 pA, $BaCl_2$ = 0.56 ± 0.4 pA, n = 8, $p = 0.05$) (**Fig. 3C**). Thus, the outward response to NA was only minimally due to activation of K^+ current but rather was mediated largely by inhibition of a tonic inward current generated by NALCN. Philippart and Khaliq (2018) observed that $GABA_B$ receptors suppressed NALCN current in substantia nigra, and so we asked whether these receptors might have a similar action in CWCs. In K^+ filled cells, puffs of the $GABA_B$ agonist baclofen generated outward currents similar to those observed with NA (**Fig 4A & C**). However, unlike NA, subsequent wash-in of $BaCl_2$ blocked 26.99 ± 4.60 % of the baclofen response (Ctrl = 42.95 ± 2.58 pA, $BaCl_2$ = 30.90 ± 1.84 pA, N = 8, $p = 0.0014$) (**Fig 4A, C & D**), suggesting the partial involvement of GIRK channels. In NALCN KO mice, the baclofen currents were significantly smaller than in wildtype (**Fig 4B&C**). Moreover, $BaCl_2$ in the KO had a much greater effect on the baclofen current, as compared to wildtype, blocking by 82.68 ± 6.71% (**Fig 4B, C & D**) (KO = 12.91 ± 3.51 pA, $BaCl_2$ = 2.57 ± 1.06 pA, N = 7, $p = 0.0089$), indicating that after loss of NALCN, the remaining baclofen response was largely dependent on GIRK channels.

Low Ca^{2+}induced inward current mediated by NALCN

NALCN current is enhanced by reduction of extracellular Ca^{2+} (Lu et al., 2007; Lu et al., 2010; Ren, 2011; Philippart and Khaliq, 2018; Chua et al., 2020), and in the presence of blockers of voltage-dependent Na^+, Ca^{2+}, and K^+ channels this effect is considered diagnostic for the presence of NALCN (Philippart and Khaliq, 2018). Recording in voltage clamp with the cocktail of intracellular and extracellular channel and receptor blockers described by Philippart and Khaliq, 2018 (see methods, and note that GIRK channels are also blocked here), an inward current of −107.61 ± 10.80 pA (N = 18) developed over several minutes upon shifting bath Ca^{2+} from 2 mM to 0.1 mM (**Fig 5A & B**). When NA was subsequently washed in, still in the presence of 0.1 mM Ca^{2+}, the inward current was immediately reduced, falling by over half (−51.14 ± 9.44 pA, N = 18) (**Fig 5A, B & F**). When similar experiments were performed in NALCN KO mice there was no change in holding current upon reduction in bath Ca^{2+}, and only a minimal current response to NA (−4.78 ± 4.66 pA, N = 6) (**Fig 5C, D & F**). In order to confirm that the reduction in inward current by NA was mediated by α2 receptors, we repeated the experiments in wildtype mice but in the presence of 1 μM idazoxan, and observed no effect on the inward current (Ctrl, 0.1 mM Ca^{2+} = −112.52 ± 12.80 pA, NA = −108.35 ± 5.80 pA, N = 5, **Fig 5E**). Additional experiments were made using baclofen to activate $GABA_B$ receptors. Here, application of 10 μM baclofen almost completely

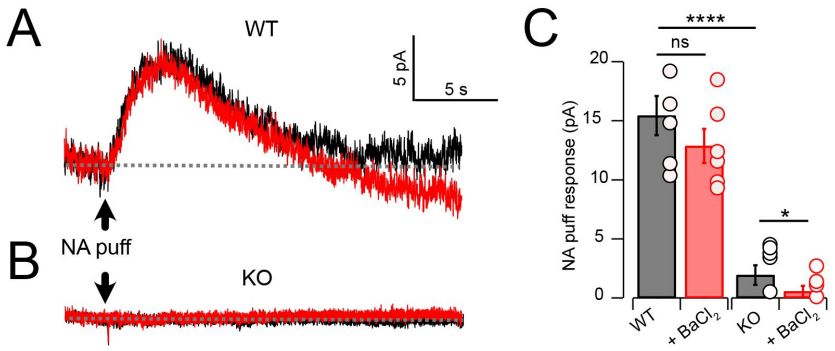

Figure 3

NA evoked a Ba^{2+}-resistant outward current that required NALCN. A, Outward current in response to NA puff (100 µM, 50 ms) in whole-cell voltage-clamp mode (−70 mV) before (black) and after (red) block of GIRK channels by bath application of 100 µM Ba^{2+}. B, As in A, but from a CWC from a NALCN KO mouse. C, Average data showing responses to NA puff in control conditions and after the block of GIRK channels from control (n =5) and NALCN KO mice (n= 6). In the KO, the NA response was markedly reduced, and was Ba^{2+} sensitive. Dashed line indicates initial current level.

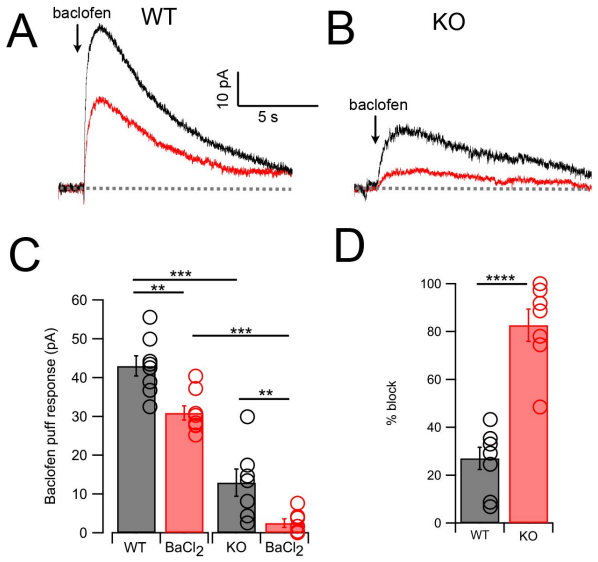

Figure 4

$GABA_B$ receptors activate outward current mediated by NALCN and GIRK channels. A, Traces from one neuron showing baclofen puff (100 µM, 50 ms) evoked outward current in control solution (black) and with 100 µM Ba^{2+} in bath (red). B, As in A but for a CWC from a NALCN KO mouse. C, Averaged data showing Ba^{2+} sensitivity of the NA response in WT and KO tissue. Ba^{2+} produced a significant block in all cases, while KO CWC showed significantly smaller baclofen responses. D, the degree of block by Ba^{2+} was significantly greater in KO mice, indicating that more of the baclofen response is mediated by GIRK channels after KO of NALCN. Dashed line indicates initial current level.

eliminated the 0.1 mM -Ca^{2+} induced NALCN current (0.1 mM Ca^{2+} = −117.75 ± 19.6 pA, baclofen = −18.80 ± 14.5 pA, N =15, p = 0.00018, **Fig 6A, C & E**), while in knockout mice, neither 0.1 mM Ca^{2+} nor baclofen altered the holding current (0.1 mM Ca^{2+} = −14.48 ± 9.39 pA, baclofen = −15.90 ± 8.94 pA, N = 6, p = 0.45, **Fig. 6B, D & E**). Altogether, these experiments support that NALCN is expressed in CWC, and generates a Ca^{2+} sensitive inward ionic current which is suppressed by α2 and $GABA_B$ receptors.

Since both NA and baclofen inhibit NALCN in CWC, we asked whether these two receptors act on independent or overlapping populations of NALCN channels. In these experiments, one set of control recordings assessed the magnitude of block by NA of low-Ca^{2+}-evoked inward current. Interleaved with these recordings were experiments in which baclofen was applied to reduce the NALCN current, and then NA subsequently applied in the continued presence of baclofen (**Fig. 7A-C**). If the two agonists act on independent populations of NALCN channels, NA should suppress inward current similar to that seen in control experiments. However, as shown in **Fig 7**, NA had virtually no blocking action of inward current following application of baclofen (0.1 mM Ca^{2+} = −164.28 ± 20.50 pA, baclofen = −53.33 ± 14.73 pA. NA = −46.94 ± 16.50 pA, N = 9, F = 41.28, p < 0.0001, repeated measures one-way ANOVA; post hoc Tukey's test, 2 mM Ca^{2+} vs 0.1 mM Ca^{2+} p = 0.002, 0.1 mM Ca^{2+} vs baclofen p = 0.005, 0.1 mM Ca^{2+} vs NA p = 0.002, baclofen vs NA p = 0.84). We also compared with percentage block of 0.1 mM Ca^{2+} current in baclofen, or NA alone, compared to the block of current by NA in a background of baclofen. Baclofen completely occluded the response to subsequent application of NA (percent block: baclofen 70.61 ± 7.18, NA 56.18 ± 9.5, additional block 4.35 ± 3.25, n = 9, $F_{(2,24)}$ = 23.83, p < 0.0001, one-way ANOVA; post hoc Tukey's test, baclofen vs NA p = 0.34, baclofen vs addition p < 0.0001, NA vs addition p < 0.0001). These data suggest that α2 receptors target the same set of NALCN channels as $GABA_B$ receptors, implying close apposition of the two receptors and the NALCN channel complex.

Noradrenergic effect not mediated by control of cAMP levels

The α2 receptor is a Gi/o GPCR and thus it is possible that inhibition of adenylyl cyclase and thus reduction of cAMP levels might mediate the action of NA on NALCN. To test this idea, CWCs were recorded in the same solutions used in the previous section, in order to block K^+ channels and other non-NALCN contributions to current. Then NA (100 μM) was puffed onto the recorded neuron, which suppresses NALCN and generates a net outward current. After recording control responses, 1 mM 8-Br-cAMP was washed into the bath, and NA responses again recorded. The average response amplitudes were 23.9±3.5 pA in control and 27.8±5.7 pA in 8-Br-cAMP (n=7 cells, p=0.1147, paired t-test). On the assumption that 8-Br-cAMP would effectively saturate cAMP actions in the neurons, the absence of an effect on the NA response suggests that inhibition cAMP production does not mediate NA action on NALCN, pointing to the possibility of direct effect of G-proteins on the channel.

Noradrenergic enhancement of glycine release

CWC mediate synaptic inhibition through the release of glycine onto fusiform principal cells as well as onto other CWC in the DCN (Mancilla and Manis, 2009; Roberts and Trussell, 2010; Kuo and Trussell, 2011; Apostolides and Trussell, 2014). NA has been shown to enhance feedforward inhibition by suppressing background spiking activity (Kuo and Trussell, 2011; Lu and Trussell, 2016). We tested more directly the effect of NA on synaptic inhibition and the role of NALCN by electrically evoking IPSCs while recording from CWC. Bipolar stimulation electrodes were positioned in the DCN molecular layer in order to stimulate CWC axons. The resulting glycinergic IPSCs were significantly enhanced upon bath application of 10 μM NA (Ctrl = −1.37 ± 0.31 nA, NA = −1.82 ± 0.43 nA, % change = 32.99 % (increase), N = 8, **Fig 8A & B**). This average increase ranged widely from 2% to 81%, suggesting some cells received glycinergic input from CWC that were not spontaneously active and therefore not affected by NA. The experiment was repeated on NALCN KO mice, there was no significant increase in IPSC amplitude (KO = −2.17± 0.54

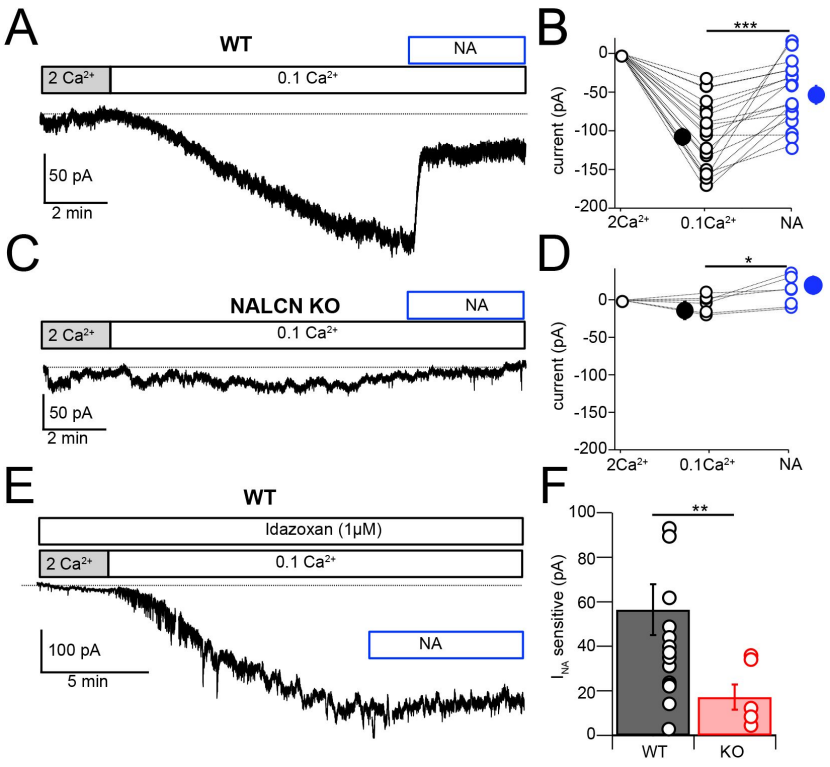

Figure 5

NALCN current evoked by Ca^{2+} reduction is inhibited by α2 receptors. A, Shifting bath Ca^{2+} from 2 mM to 0.1 mM evokes a slow inward current that is then rapidly reduced by subsequent wash-in of 10 μM NA. B, Group data showing the magnitude of inward current shift in 0.1 mM Ca^{2+} (black) and the significantly smaller shift in 0.1 mM Ca^{2+} plus NA (blue). N= 18 cells. C, Experiment as in A but for a CWC from a NALCN KO mouse. D, As in B, but for CWC from KO tissue. N=6 cells. E, Experiment as in A but in continuous presence of 1 μM idazoxan. NA failed to block the low-Ca^{2+} evoked current. F, The magnitude of inward current blocked by NA was significantly greater in WT as compared to KO cells. All neurons voltage clamped to −70 mV. Statistical significance: * $p < 0.05$; ** $p < 0.01$; *** $p < 0.001$. Extracellular solution contained TTX, NBQX, MK-801, strychnine, SR95331, apamin. Dashed line indicates initial current level.

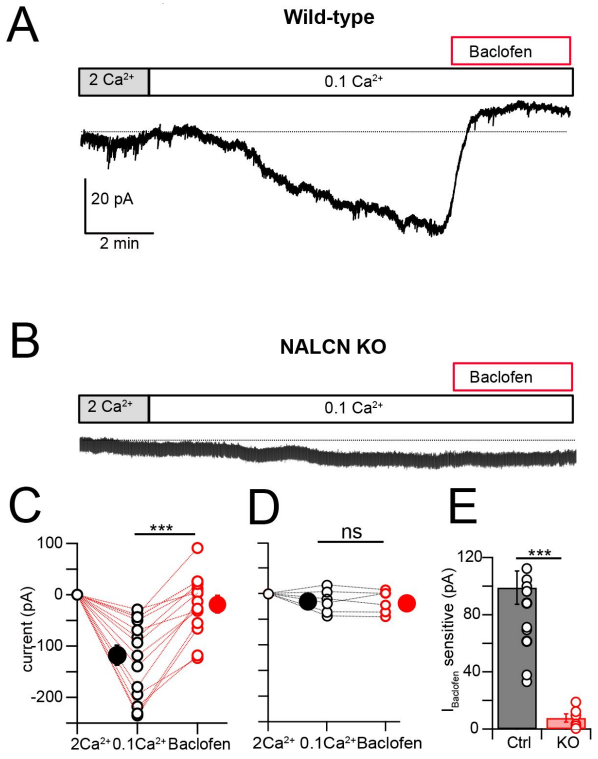

Figure 6

NALCN current evoked by Ca^{2+} reduction is inhibited by $GABA_B$ receptors. A, Shifting bath $Ca^{2+}$from 2 mM to 0.1 mM evokes a slow inward current that is then rapidly reduced by subsequent wash-in of 10 μM baclofen. B, Experiment as in A but for a CWC from a NALCN KO mouse. C, Group data showing the magnitude of inward current shift in 0.1 mM Ca^{2+} (black) and the significantly smaller shift in 0.1 mM Ca^{2+} plus baclofen (red). N= 18 cells. D, As in C, but for CWC from KO tissue. N=6 cells. E, The magnitude of inward current blocked by baclofen was significantly greater in WT as compared to KO cells. All neurons voltage clamped to −70 mV. Statistical significance: * $p < 0.05$; ** $p < 0.01$; *** $p < 0.001$. Extracellular solution contains TTX, NBQX, MK-801, strychnine, SR95331, apamin. Dashed line indicates initial current level.

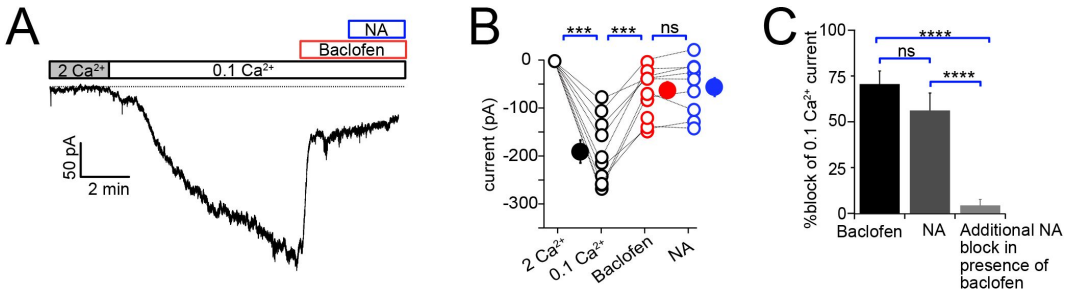

Figure 7

Baclofen and NA act on the same population of NALCN channels. A, Representative example of NALCN current evoked by shift from 2 mM Ca^{2+} to 0.1 mM Ca^{2+}, followed by bath application of baclofen (20 μM) and subsequent application of NA (10 μM) with baclofen still present. In the presence of baclofen, the rapid decline in inward current normally evoked by NA was absent. B, Summary plot of NALCN current amplitude evoked by 0.1 mM Ca^{2+} and after baclofen and subsequent NA application (WT, N = 9). NA failed to produce a significant change after baclofen application. C, Percentage block of 0.1 Ca^{2+} current in baclofen, or NA alone, compared to the block of current by NA in a background of baclofen. Baclofen completely occluded response to subsequent application of NA. Statistical significance, *** $p < 0.001$. Dashed line indicates initial current level.

nA, NA = −2.08 ± 0.55 nA, % change = 3.77% (decrease), N = 10, p = 0.0011; **Fig 8 B & C**). Thus, NA-mediated increase in the strength of inhibition (Kuo and Trussell, 2011) is likely mediated by NALCN.

Discussion

Mechanism of adrenergic modulation

The primary effect of noradrenergic modulation of the CWC is to enhance the strength of inhibitory synaptic transmission (Kuo and Trussell, 2011). Modulation by NA acts simultaneously on all the CWC neurons synapses by impacting spike generation and thereby the degree of frequency-dependent synaptic depression. We show here that NALCN is the ion channel that mediates this effect on firing. α2 receptors are known to mediate inhibition of firing through enhancement of K^+ channel activity, and GIRK channels play a prominent role in these effects (Williams et al., 1985; Aghajanian and Wang, 1986; Arima et al., 1998; Li and van den Pol, 2005). However, in CWC, almost none of the effect of NA was blocked by the K^+ channel blocker Ba^{2+}. Indeed, since in NALCN KOs the NA-induced effects on spiking, outward currents or block of inward currents were all eliminated, it is almost certain that NALCN and not K^+ channels play the key role in noradrenergic modulation in CWC. A caveat is that we only examined ionic currents and voltage changes measurable with a somatic electrode. NA effects in distal dendrites may have been undetectable at the soma.

Several intriguing aspects of NA action are revealed in this work when considered together with our previous study (Kuo and Trussell, 2011). First, the action NA on feedforward inhibition is apparently quite specific to NALCN. No effect of NA was observed on parallel fiber EPSCs in CWC or CWC IPSCs in fusiform cells recorded during paired voltage-clamp recordings (Kuo and Trussell, 2011). This suggests that the mechanism for control of inhibitory strength is optimized to act globally on the CWC's synapses by controlling spontaneous firing. Presumably, α2 receptors are localized in such a way to affect membrane potential and rheobase at the soma and/or at the axon initial segment, although localization studies will be required to address this uncertainty. Despite the DCN's dense innervation from noradrenergic fibers (Kromer and Moore, 1980; Klepper and Herbert, 1991), we do not know the morphology of noradrenergic synapses in the DCN. However, if NA release is through "volume transmission", it may be that noradrenergic modulation acts on groups of CWCs and all their synapses. Second, although CWC have GIRK channels, and α2 activate GIRK channels in some other neuronal cell types (Arima et al., 1998; Paladini and Williams, 2004; Li and van den Pol, 2005), the CWC has selected for a mechanism in which an inhibitory action is associated with a decrease in a tonic membrane conductance. The effect on membrane potential of this decrease in conductance is small, ~2 mV. Yet, we show that that shift alone is sufficient to profoundly inhibit spontaneous firing and thereby increase the strength of inhibitory synapses. Interestingly, an inverse mechanism of modulation was described in hippocampus, in which oxytocin increases spontaneous firing of interneurons and thus decreases inhibitory synaptic strength (Owen et al., 2013). In this case oxytocin acts by decrease of a resting inhibitory conductance mediated by Kv7 channels (Tirko et al., 2018). Thus, modulation by inhibitory or excitatory conductance decrease provides a means for global control of inhibitory synaptic strength in the CNS.

Convergence of GABAergic and adrenergic systems

Unlike α2 receptors, the actions of $GABA_B$ receptors were more complex, as $GABA_B$ receptors both inhibited NALCN and activated GIRK channels, as previously observed in substantia nigra neurons (Philippart and Khaliq, 2018). Comparisons of the magnitude of NA action in control recordings and in a background of baclofen indicated that the two modulators acted on a common population of NALCN channels. While activation of α2 receptors may lead to inhibition of adenylyl cyclase (Dohlman, et al. 1987), we did not observe an effect of 8-Br-cAMP on NA responses, arguing

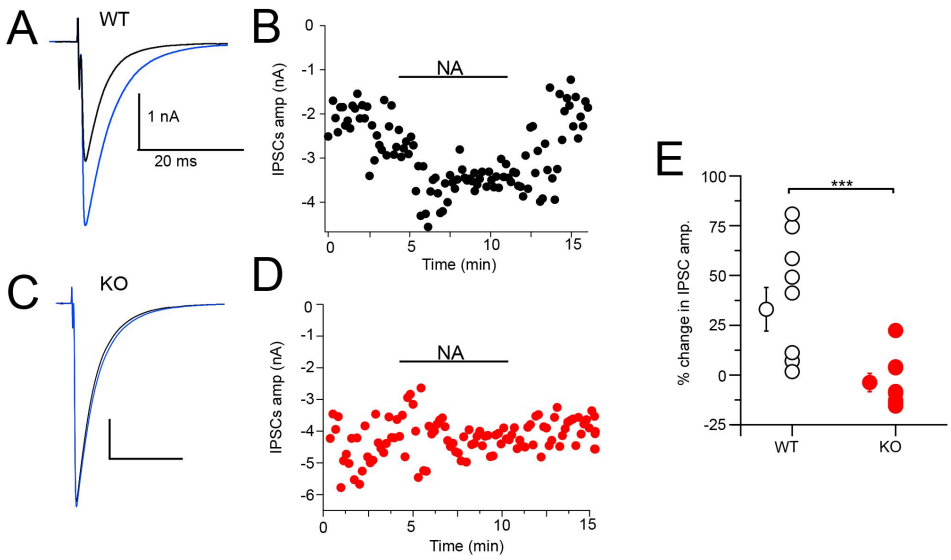

Figure 8

NA enhances CWC-mediated IPSCs in WT but not NALCN CWC KO. A, Example average trace of evoked IPSCs recorded from a CWC with a CsCl pipette fill, before (black) and after (blue) bath application of 10 μM NA. B, Diary plot of effect of NA application (applied during black bar) of the IPSCs amplitude in cell A. C, Example average trace of evoked IPSCs recorded from a CWC as in A, but from a NALCN KO mouse. Data shown before (black) and after (blue) bath application of 10 μM NA. D, Diary plot of effect of NA application in C. E, Summary plot of percent change of IPSCs amplitude after NA application in WT and KO mice. (WT, N = 8; KO, N = 10)

against a role for cAMP. If gating of the channels proceeds directly by membrane-delimited actions of G-proteins, it is likely that a pool of $GABA_B$ and α2 receptors are in relatively close apposition to one another and to NALCN. However, unlike $GABA_B$ receptors, α2 receptors did not appreciably activate GIRK channels. Altogether, these results suggest two distinct pools of $GABA_B$ receptors in the somatodendritic membrane: one associated with GIRK and one with NALCN. In addition, a third pool is localized in CWC nerve terminals. There, baclofen suppresses release of action potential-independent exocytosis (Apostolides and Trussell, 2013), suggesting modulation by $GABA_B$ receptors of Ca^{2+} channels or exocytic proteins. Regarding the somatodendritic populations, immunolocalization with electron microscopy indicated that GABAB1 subunits are concentrated at the base of dendritic spines of CWC, rather than associated with GABAergic synapses (Lujan et al., 2004), with the suggestion that they respond to "spillover" of GABA. It remains unclear which ion channel this particular dendritic $GABA_B$ population modulates.

Auditory processing

The DCN is the site of diverse forms of neuromodulation mediated by G-protein coupled receptors (Trussell and Oertel, 2018; Trussell, 2019), in which transmitters act at presynaptic membrane to regulate exocytosis (Tang and Trussell, 2015, 2017), at the axon initial segment to control spike pattern (Bender et al., 2010), at somatodendritic membrane to boost firing (Tang and Trussell, 2017), or at dendritic spines to control postsynaptic efficacy (He et al., 2014). By restricting α2 modulation to the spike-generation mechanism and not presynaptic release zones, the transmitter is able to enhance IPSC amplitude while simultaneously reducing background inhibitory "noise", thus enhancing the salience of a given interneuron's impact. CWC are activated by parallel fibers conveying multisensory input to DCN fusiform cells. If, consistent with other studies (Berridge and Waterhouse, 2003), NA is released during brain states associated with wakefulness, this enhanced signal-to-noise mediated by NA would serve to more precisely sculpt the output of DCN based on such multisensory signals. Moreover, since individual CWC-fusiform synaptic pairs apparently receive excitatory input from different populations of parallel fibers (Roberts and Trussell, 2010), such enhanced inhibition might serve a more precise computational role that a standard feedforward inhibitory mechanism. NALCN therefore appears to play a potent role in selective sensory filtering during heightened states of vigilance.

Materials and Methods

Key Resources Table				
Reagent type (species) or resource	**Designation**	**Source or reference**	**Identifiers**	**Additional information**
strain, strain background (*M musculus*)	C57BL/6J	Jackson Laboratory	RRID: JAX:000664	
strain, strain background (*M musculus*)	GlyT2-EGFP, Tg(Slc6a5-EGFP)1Uze	MGI, Zeilhofer et al., 2005	RRID: MGI:3835459	
strain, strain background (*M musculus*)	B6(Cg)-*Nalcn*$^{tm1c(KOMP)Wtsi}$/DrenJ	MGI and Jackson Laboratory	RRID: JAX_030718	
strain, strain background (*M musculus*)	Slc6a5$^{tm1.1(cre)Ksak}$ (GlyT2Cre)	MGI	RRID: MGI:6382286	

Chemical compound, drug	Strychnine hydrochloride	Sigma	Cat# S8753	
Chemical compound, drug	SR-95531 hydrobromide	Tocris	Cat# 1262	
Chemical compound, drug	NBQX disodium salt	Tocris	Cat# 1044	
Chemical compound, drug	(+)-MK-801 hydrogen maleate	Sigma	Cat# M107	
Chemical compound, drug	L-(-)-Norepinephrine (+)-bitartrate salt monohydrate	Sigma	Cat# A9512	
Chemical compound, drug	(±)-Norepinephrine (+)-bitartrate salt	Sigma	Cat# A0937	
Chemical compound, drug	Idazoxan hydrochloride	Sigma	Cat# I6138-100MG	
Chemical compound, drug	Apamin	Alomone Labs	Cat# STA-200	

Chemical compound, drug	D-AP5	Tocris	Cat# 0106	
Chemical compound, drug	Barium Chloride	Sigma	Cat# 202738	
Software, algorithm	pClamp 10	Molecular Devices	RRID:SCR_011323	
Software, algorithm	Igor Pro 8	WaveMetrics	RRID:SCR_000325	
Software, algorithm	NeuroMatic	Rothman and Silver, 2018; DOI:10.3389	RRID:SCR_004186	
Software, algorithm	Axograph	Axograph	RRID:SCR_014284	
Software, algorithm	Prism 9	GraphPad	RRID:SCR_002798	
Software, algorithm	Excel	Microsoft	RRID:SCR_016137	
Software, algorithm	Affinity Designer	Serif	RRID:SCR_016952	

Animals

All procedures were approved by the Oregon Health and Science University's Institutional Animal Care and Use Committee. C57BL/6J, GlyT2-EGFP mice (Zeilhofer et al., 2005; Ngodup et al., 2020), and NALCN conditional knock mice of either sex, postnatal days (P) 17–40 were used in this study. GlyT2-GFP mice were backcrossed into the C57BL/6J and maintained as heterozygous. As global knockout of NALCN is lethal, we generated a glycinergic neuron-specific knock out by crossing NALCN$^{flox/flox}$ mice (B6(Cg)-Nalcn$^{tm1c(KOMP)Wtsi}$/DrenJ) with GlyT2-Cre mice (Tg(Slc6a5-cre)1Uze), resulting in NALCN^{flox};GlyT2-Cre offspring. The F1 litters were back crossed with NALCN$^{flox/flox}$ mice to generate NALCN$^{flox/flox}$;GlyT2-Cre that lack NALCN expression in glycinergic cells. NALCN conditional knock out mice were smaller than age matched WT litters but had normal hearing as established by auditory brainstem response.

Brain-slice preparation

Animals were anesthetized with isoflurane and decapitated. The brain was quickly removed and placed into ice-cold sucrose cutting solution. Sucrose solution contained (in mM) 76 NaCl, 26 $NaHCO_3$, 75 sucrose, 1.25 NaH_2PO_4, 2.5 KCl, 25 glucose, 7 $MgCl_2$, and 0.5 $CaCl_2$, bubbled with 95% O_2: 5% CO_2 (pH 7.8, 305 mOsm). Coronal slices containing DCN were cut at 210 µm in ice-cold sucrose solution on a vibratome ((VT1200S; Leica Microsystems, Wetzlar, Germany) or (7000smz-2; Campden Instruments, Loughborough, UK)). Slices were transferred into standard artificial

cerebrospinal fluid (ACSF) containing (in mM) 125 NaCl, 20 $NaHCO_3$, 1.2 KH_2PO_4, 3 HEPES, 2.1 KCl, 20 glucose, 1 $MgCl_2$, 1.2 $CaCl_2$, 2 Na-pyruvate, and 0.4 Na L-ascorbate, bubbled with 95% O_2:5% CO_2 (pH 7.4, 300–310 mOsm). Slices were recovered at 34°C for 40 min and were maintained at room temperature until recording.

Electrophysiology

Slices were transferred to a recording chamber and perfused with standard ACSF at 3 ml/min and maintained at 31-34°C with an in-line heater (TC-324B; Warner Instruments, Hamden, CT). Cells were viewed using an upright microscope (BX51WI; Olympus, Tokyo, Japan) with a 60X objective, equipped with an infrared custom-made Dodt contrast, CCD camera (Retiga 2000R; QImaging, Surrey, Canada), and fluorescence optics. All recordings were collected from CWCs of the DCN. CWCs were targeted by their location in the molecular and fusiform cell layers of DCN, and by their round soma (Kim and Trussell, 2007). Identification was then confirmed by their distinctive firing pattern (simple or complex spikes) (Golding and Oertel, 1997). In slices from GlyT2-EGFP, glycinergic cells in the DCN were identified by their GFP expression. In some experiments, 0.1% biocytin (B1592; Thermo Fisher Scientific, Waltham, MA) was added to the pipette solution for post-hoc identification of CWCs. Recording pipettes were pulled from 1.5 mm OD, 0.84 mm ID borosilicate glass (1B150-F; World Precision Instruments, Sarasota, FL) to a resistance of 2–4 MΩ using a horizontal puller (P-97 or P-1000; Sutter Instruments, Novato, CA). In most experiments, internal recording solution contained in (mM) 113 K gluconate, 2.75 $MgCl_2$, 1.75 $MgSO_4$, 0.1 EGTA, 14 $Tris_2$-phosphocreatine, 4 Na_2-ATP, 0.3 Tris-GTP, 9 HEPES with pH adjusted to 7.25 with KOH, mOsm adjusted to 290 with sucrose (E_{Cl}, −84 mV). For voltage clamp to isolate NALCN current, internal solution contained in (mM) 87 $CsMeSO_3$, 18 CsCl, 5 CsF, 10 TEA-Cl, 10 HEPES, 5 EGTA, 5 Mg-ATP, 0.3 Na_2-GTP, 13 di-Na phosphocreatine, 2 QX-314 (pH 7.25, 295 mOsm). For a few voltage-clamp experiments, we used an internal solution containing (in mM) 103 CsCl, 10 TEA-Cl, 2.75 $MgCl_2$, 9 HEPES, 0.1 EGTA, 0.3 Tris-GTP, 14 $Tris_2$-phosphocreatine, 4 Na_2-ATP, 3.5 QX-314 (pH adjusted to 7.2 with CsOH). Puff application of agonists and antagonists was delivered through a picospritzer (Picospritzer III; Toohey Company, Fairfield, NJ), at 7-10 psi, with borosilicate glass capillaries. NA or Baclofen applications were at 100 µM and 5-10 ms in duration. The puff pipette was placed around 100 µm from the soma of the recorded cell to avoid mechanical disturbance.

Cell-attached (voltage-clamp) recordings were made using normal extracellular solution. Whole-cell patch-clamp recordings were made using a Multiclamp 700B amplifier and pCLAMP 10 software (Molecular Devices; Sunnyvale, CA). Signals were digitized at 20–40 kHz and filtered at 10 kHz by Digidata 1440A (Molecular Devices). In voltage clamp, cells were held at −65 mV, with access resistance 5-30 MΩ compensated to 40– 60%. In current clamp with control solutions, the resting membrane potential was maintained at −60 to −70 mV with bias current. To isolate NALCN currents, synaptic blockers, NBQX (10 µM), MK-801 (10 µM), SR-95531 (10 µM) or picrotoxin (100 µM), strychnine (0.5 µM), apamin (100 nM), and $BaCl_2$ (200 µM) were added to the bath solution. In those experiments, shifts in Ca^{2+} from 2 mM to 0.1 mM were accompanied by a shift in Mg^{2+} from 1 mM to 3 mM. To record evoked IPSCs, CWCs were stimulated with brief voltage pulses (100 µs) using a stimulus isolation unit (Iso-Flex; A.M.P.I, Jerusalem, Israel) via a glass microelectrode placed in the molecular layer of the DCN.

Pharmacology

All drugs in the slice experiments were bath applied. Receptor antagonists used in this study included: NBQX (AMPA receptors; Sigma-Aldrich, St. Louis, MO), MK-801 (NMDA receptors; Sigma-Aldrich), SR-95531 ($GABA_A$R; Tocris Bioscience, Bristol, UK), strychnine (glycine receptors; Sigma-Aldrich).

ABRs

Auditory brainstem responses (ABR) were acquired from C57B6/J and NALCN KO mice between P40-50. Mice were anesthetized with a dose of 80 mg/kg ketamine:16 mg/kg xylazine. ABRs were recorded differentially with electrodes at the vertex and pinna with ground at the base of the tail. Tone pips (5 msec, 0.5 msec rise/fall with 4-msec steady-state plateau) were generated digitally with a PXI-4461 card (National Instruments, Austin, TX), amplified (SA1; Tucker-Davis Technologies, Alachua, FL) and delivered using a compact, close-field sound system consisting of two CUI earphones and an electric microphone (FG-23329-P07; Knowles, Itasca, IL) coupled to a probe tube (Buran, 2015; Hancock K et al., 2015; Buran et al., 2020). Tone levels were incremented in 5-dB steps from 0 to 90-dB SPL. ABRs were recorded in a sound-proof booth using a Grass P511 amplifier and digitized using a National Instruments PXI 4661 card. ABR threshold was obtained for each animal. ABR peaks and thresholds were identified by visual inspection of the waveforms in a custom-written analysis program (Buran, 2015). Body temperature was maintained between 36 and 37°C using a homeothermic blanket (Harvard Apparatus, Cambridge, MA).

Experimental design and statistical analyses

Electrophysiological data were analyzed using pClamp 10.4 software (Molecular Devices), Axograph, or IGOR Pro v6.3 or v8 (WaveMetrics, Lake Oswego, OR) and NeuroMatic (Rothman and Silver, 2018).Figures were made using IGOR Pro, Affinity Designer, and Adobe Illustrator. Statistics were performed in IGOR Pro, Axograph, Python, Microsoft Excel, or Prism 7 (GraphPad, San Diego, CA). Error bars are represented as mean ± SEM unless otherwise stated.

Acknowledgements

This work was supported by NIH grants R35NS116798 and DC004450 to L.O.T. and JSPS KAKENHI Grant Number 22K06838 to T.I. We thank Drs. John Williams and members of the Trussell Lab for comments.

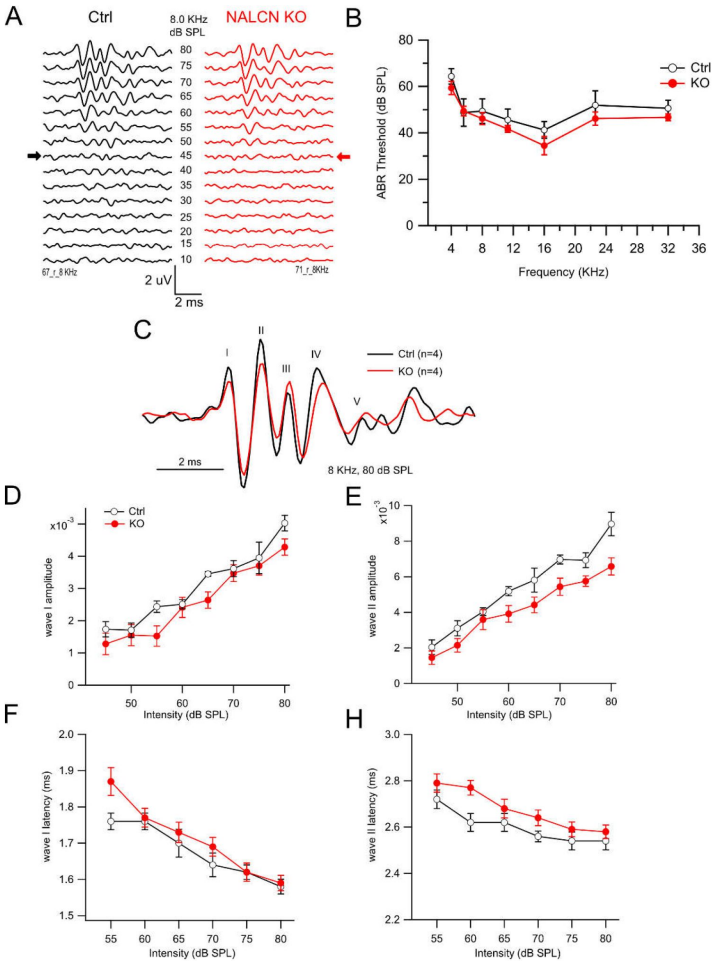

Figure 1-figure supplement 1

NALCN KO mice show no difference in auditory brainstem response (ABR) from wildtype (WT). A. Example traces of WT (left) and NALCN KO (right: red) ABR responses to 8 KHz pure tones presented at different sound intensities. Arrows indicate ABR wave I threshold. B. ABR thresholds for WT and NALCN KO mice were similar for various pure tones tested for mouse hearing ($p > 0.95$ for all frequencies, ANOVA/Sidak's multiple comparison test). C. Example ABR trace from WT (black) and NALCN KO (red) in response to 8 KHz pure tone at 80 dB SPL. D-H, Maximum wave I and II amplitude (D, F) and latencies (E, H) to 8 KHz tone stimulation presented at 80 dB SPL were not different between WT (N = 4) and NALCN KO animals (N = 4).

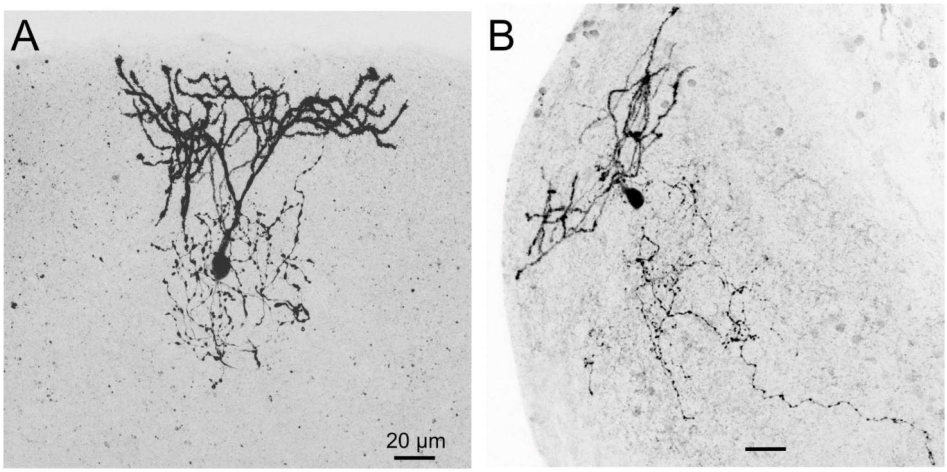

Figure 1-figure supplement 2

Biocytin-filled CWCs from NALCN KO mice. A, B, Two examples of CWC that were labeled with biocytin imaged using confocal microscopy. Characteristic of CWC, spiny dendrites extend up to the ependymal layer while a fine axon ramifies within the molecular and cell body layers of the DCN.

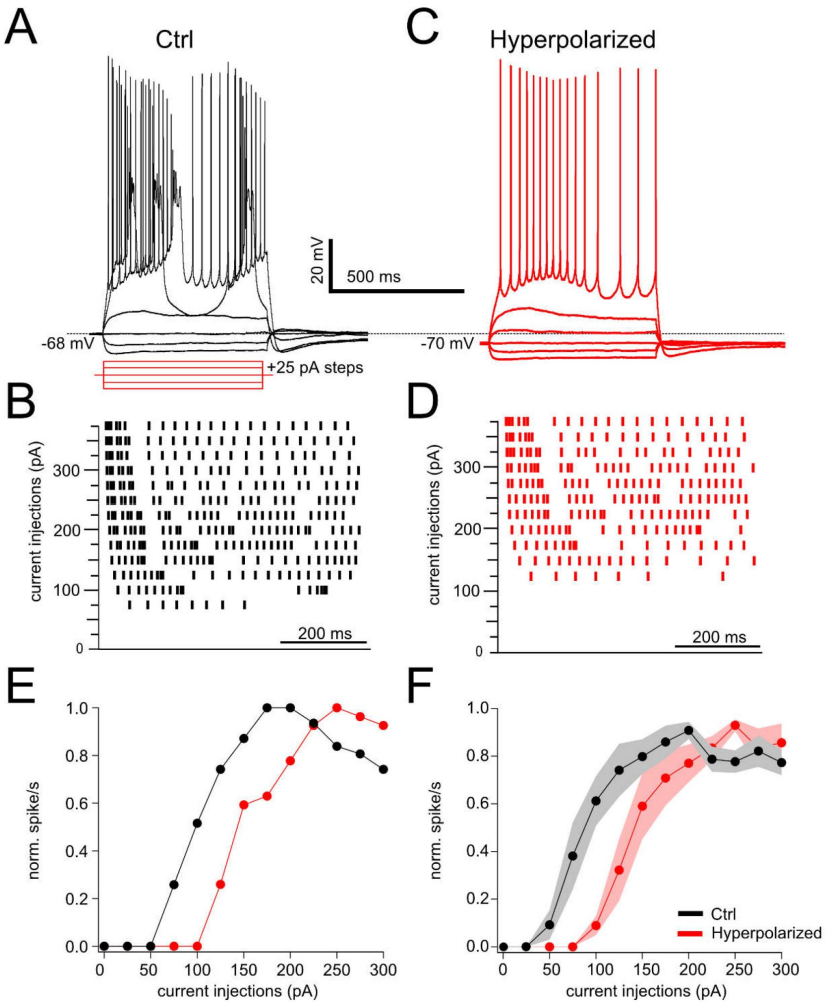

Figure 2-figure supplement 1

NA effect on rheobase and spiking is voltage dependent. A, Profile of voltage responses to current steps. Simple and complex spikes evoked in response to depolarizing current steps. B. Raster plot of spike timings during different level of current injection. C, D same cell as in B but membrane hyperpolarized by 2 mV (see dashed line). E, Normalized spike rate plotted as function of current level of cell A and C. F, Average data for spike rate from ctrl and bias current injected conditions. Hyperpolarizing current injection show increase in rheobase and suppression of evoked firing (rheobase ctrl = 70.88 ± 7.68 pA, hyperpolarized = 125 ± 12.90 pA, N = 6, p = 0.0009).

References

Aghajanian GK, Wang YY (1986) **Pertussis toxin blocks the outward currents evoked by opiate and alpha 2-agonists in locus coeruleus neurons** *Brain Res* **371**:390–394

Al-Sayed MD *et al.* (2013) **Mutations in NALCN cause an autosomal-recessive syndrome with severe hypotonia, speech impairment, and cognitive delay** *Am J Hum Genet* **93**:721–726

Apostolides PF, Trussell LO (2013) **Rapid, activity-independent turnover of vesicular transmitter content at a mixed glycine/GABA synapse** *J Neurosci* **33**:4768–4781

Apostolides PF, Trussell LO (2014) **Control of interneuron firing by subthreshold synaptic potentials in principal cells of the dorsal cochlear nucleus** *Neuron* **83**:324–330

Arima J, Kubo C, Ishibashi H, Akaike N (1998) **alpha2-Adrenoceptor-mediated potassium currents in acutely dissociated rat locus coeruleus neurones** *J Physiol* **508**:57–66

Bender KJ, Trussell LO (2009) **Axon initial segment Ca2+ channels influence action potential generation and timing** *Neuron* **61**:259–271

Bender KJ, Ford CP, Trussell LO (2010) **Dopaminergic modulation of axon initial segment calcium channels regulates action potential initiation** *Neuron* **68**:500–511

Berridge CW, Waterhouse BD (2003) **The locus coeruleus-noradrenergic system: modulation of behavioral state and state-dependent cognitive processes** *Brain Res Brain Res Rev* **42**:33–84

Bramswig NC, et al. (2018) **Genetic variants in components of the NALCN-UNC80-UNC79 ion channel complex cause a broad clinical phenotype (NALCN channelopathies)** *Hum Genet* **137**:753–768

Buran BN (2015) **Buran BN (2015) Auditory-wave-analysis: V1.1. Zenodo https://zenodoorg/record/17365** *Auditory-wave-analysis: V1.1. Zenodo*

Buran BN, Elkins S, Kempton JB, Porsov EV, Brigande JV, David SV (2020) **Optimizing Auditory Brainstem Response Acquisition Using Interleaved Frequencies** *J Assoc Res Otolaryngol* **21**:225–242

Chong JX, et al. (2015) **De novo mutations in NALCN cause a syndrome characterized by congenital contractures of the limbs and face, hypotonia, and developmental delay** *Am J Hum Genet* **96**:462–473

Chua HC, Wulf M, Weidling C, Rasmussen LP, Pless SA (2020) **The NALCN channel complex is voltage sensitive and directly modulated by extracellular calcium** *Sci Adv* **6**

Cochet-Bissuel M, Lory P, Monteil A (2014) **The sodium leak channel, NALCN, in health and disease** *Front Cell Neurosci* **8**

Dohlman HG, Caron MG, Lefkowitz RJ (1987) **A family of receptors coupled to guanine nucleotide regulatory proteins** *Biochemistry* **26**:2657–2664

Golding NL, Oertel D (1997) **Physiological identification of the targets of cartwheel cells in the dorsal cochlear nucleus** *J Neurophysiol* **78**:248–260

Hancock K, Stefanov-Wagner IJ, Ravicz ME MC L (2015) **The Eaton-Peabody Laboratories Cochlear Function Test Suite** *Association for Research in otolaryngology 38th annual midwinter meeting*

He S, Wang YX, Petralia RS, Brenowitz SD (2014) **Cholinergic modulation of large-conductance calcium-activated potassium channels regulates synaptic strength and spine calcium in cartwheel cells of the dorsal cochlear nucleus** *J Neurosci* **34**:5261–5272

Kim Y, Trussell LO (2007) **Ion channels generating complex spikes in cartwheel cells of the dorsal cochlear nucleus** *J Neurophysiol* **97**:1705–1725

Klepper A, Herbert H (1991) **Distribution and origin of noradrenergic and serotonergic fibers in the cochlear nucleus and inferior colliculus of the rat** *Brain Res* **557**:190–201

Kromer LF, Moore RY (1980) **Norepinephrine innervation of the cochlear nuclei by locus coeruleus neurons in the rat** *Anat Embryol (Berl* **158**:227–244

Kschonsak M *et al.* (2020) **Structure of the human sodium leak channel NALCN** *Nature* **587**:313–318

Kuo SP, Trussell LO (2011) **Spontaneous spiking and synaptic depression underlie noradrenergic control of feed-forward inhibition** *Neuron* **71**:306–318

Kuo SP, Lu HW, Trussell LO (2012) **Intrinsic and synaptic properties of vertical cells of the mouse dorsal cochlear nucleus** *J Neurophysiol* **108**:1186–1198

Li Y, van den Pol AN (2005) **Direct and indirect inhibition by catecholamines of hypocretin/orexin neurons** *J Neurosci* **25**:173–183

Lu B, Su Y, Das S, Liu J, Xia J, Ren D (2007) **The neuronal channel NALCN contributes resting sodium permeability and is required for normal respiratory rhythm** *Cell* **129**:371–383

Lu B, Zhang Q, Wang H, Wang Y, Nakayama M, Ren D (2010) **Extracellular calcium controls background current and neuronal excitability via an UNC79-UNC80-NALCN cation channel complex** *Neuron* **68**:488–499

Lu HW, Trussell LO (2016) **Spontaneous Activity Defines Effective Convergence Ratios in an Inhibitory Circuit** *J Neurosci* **36**:3268–3280

Lu TZ, Feng ZP (2011) **A sodium leak current regulates pacemaker activity of adult central pattern generator neurons in Lymnaea stagnalis** *PLoS One* **6**

Lujan R, Shigemoto R, Kulik A, Juiz JM (2004) **Localization of the GABAB receptor 1a/b subunit relative to glutamatergic synapses in the dorsal cochlear nucleus of the rat** *J Comp Neurol* **475**:36–46

Luscher C, Jan LY, Stoffel M, Malenka RC, Nicoll RA (1997) **G protein-coupled inwardly rectifying K+ channels (GIRKs) mediate postsynaptic but not presynaptic transmitter actions in hippocampal neurons** *Neuron* **19**:687–695

Lutas A, Lahmann C, Soumillon M, Yellen G (2016) **The leak channel NALCN controls tonic firing and glycolytic sensitivity of substantia nigra pars reticulata neurons** *Elife* **5**

Mancilla JG, Manis PB (2009) **Two distinct types of inhibition mediated by cartwheel cells in the dorsal cochlear nucleus** *J Neurophysiol* **102**:1287–1295

May BJ (2000) **Role of the dorsal cochlear nucleus in the sound localization behavior of cats** *Hear Res* **148**:74–87

Nash HA, Scott RL, Lear BC, Allada R (2002) **An unusual cation channel mediates photic control of locomotion in Drosophila** *Curr Biol* **12**:2152–2158

Ngodup T, Romero GE, Trussell LO (2020) **Identification of an inhibitory neuron subtype, the L-stellate cell of the cochlear nucleus** *Elife* **9**

Nimitvilai S, Lopez MF, Mulholland PJ, Woodward JJ (2017) **Ethanol Dependence Abolishes Monoamine and GIRK (Kir3) Channel Inhibition of Orbitofrontal Cortex Excitability** *Neuropsychopharmacology* **42**:1800–1812

Oertel D, Young ED (2004) **What's a cerebellar circuit doing in the auditory system?** *Trends Neurosci* **27**:104–110

Owen SF, Tuncdemir SN, Bader PL, Tirko NN, Fishell G, Tsien RW (2013) **Oxytocin enhances hippocampal spike transmission by modulating fast-spiking interneurons** *Nature* **500**:458–462

Paladini CA, Williams JT (2004) **Noradrenergic inhibition of midbrain dopamine neurons** *J Neurosci* **24**:4568–4575

Philippart F, Khaliq ZM (2018) **G(i/o) protein-coupled receptors in dopamine neurons inhibit the sodium leak channel NALCN** *Elife* **7**

Ren D (2011) **Sodium leak channels in neuronal excitability and rhythmic behaviors** *Neuron* **72**:899–911

Roberts MT, Trussell LO (2010) **Molecular layer inhibitory interneurons provide feedforward and lateral inhibition in the dorsal cochlear nucleus** *J Neurophysiol* **104**:2462–2473

Rothman JS, Silver RA (2018) **NeuroMatic: An Integrated Open-Source Software Toolkit for Acquisition, Analysis and Simulation of Electrophysiological Data** *Front Neuroinform* **12**

Shi Y *et al.* (2016) **Nalcn Is a "Leak" Sodium Channel That Regulates Excitability of Brainstem Chemosensory Neurons and Breathing** *J Neurosci* **36**:8174–8187

Tang ZQ, Trussell LO (2015) **Serotonergic regulation of excitability of principal cells of the dorsal cochlear nucleus** *J Neurosci* **35**:4540–4551

Tang ZQ, Trussell LO (2017) **Serotonergic Modulation of Sensory Representation in a Central Multisensory Circuit Is Pathway Specific** *Cell reports* **20**:1844–1854

Tirko NN, Eyring KW, Carcea I, Mitre M, Chao MV, Froemke RC, Tsien RW (2018) **Oxytocin Transforms Firing Mode of CA2 Hippocampal Neurons** *Neuron* **100**:593–608

Trussell LO, Kandler K (2019) **In Vitro Studies of Neuromodulation and Plasticity in the Dorsal Cochlear Nucleus** *Oxford Handbook of the Auditory System* :123–143

Trussell LO, Oertel D (2018) **Trussell LO, Oertel D (2018) Microcircuits of the Dorsal Cochlear Nucleus. The Mammalian Auditory Pathways: Synaptic Organization and Microcircuits 65.** *Microcircuits of the Dorsal Cochlear Nucleus. The Mammalian Auditory Pathways: Synaptic Organization and Microcircuits* **65**

Williams JT, Henderson G, North RA (1985) **Characterization of alpha 2-adrenoceptors which increase potassium conductance in rat locus coeruleus neurones** *Neuroscience* **14**:95–101

Xie J, Ke M, Xu L, Lin S, Huang J, Zhang J, Yang F, Wu J, Yan Z (2020) **Structure of the human sodium leak channel NALCN in complex with FAM155A** *Nat Commun* **11**

Xie L, Gao S, Alcaire SM, Aoyagi K, Wang Y, Griffin JK, Stagljar I, Nagamatsu S, Zhen M (2013) **NLF-1 delivers a sodium leak channel to regulate neuronal excitability and modulate rhythmic locomotion** *Neuron* **77**:1069–1082

Zeilhofer HU, Studler B, Arabadzisz D, Schweizer C, Ahmadi S, Layh B, Bosl MR, Fritschy JM (2005) **Glycinergic neurons expressing enhanced green fluorescent protein in bacterial artificial chromosome transgenic mice** *J Comp Neurol* **482**:123–141

Article and author information

Tenzin Ngodup
Oregon Hearing Research Center and Vollum Institute, Oregon Health & Science University, Portland OR USA
ORCID iD: 0000-0002-9034-2957

Tomohiko Irie
Department of Physiology, Kitasato University School of Medicine, Sagamihara, Japan
ORCID iD: 0000-0002-8441-8417

Sean Elkins
Oregon Hearing Research Center and Vollum Institute, Oregon Health & Science University, Portland OR USA

Laurence O. Trussell
Oregon Hearing Research Center and Vollum Institute, Oregon Health & Science University, Portland OR USA
For correspondence: trussell@ohsu.edu
ORCID iD: 0000-0003-1171-2356

Copyright

Editors

Reviewer #1 (Public Review):

This study uses electrophysiological techniques in vitro to address the role of the Na+ leak channel NALCN in various physiological functions in cartwheel interneurons of the dorsal cochlear nucleus. Comparing wild type and glycinergic neuron-specific knockout mice for NALCN, the authors show that these channels 1) are required for spontaneous firing, 2) are modulated by noradrenaline (NA, via alpha2 receptors) and GABA (through GABAB receptors), 3) how the modulation by NA enhances IPSCs in these neurons.

This work builds on previous results from the Trussell's lab in terms of the physiology of cartwheel cells, and from other labs in terms of the role of NALCN channels, that have been characterized in more and more brain areas somewhat recently; for this reason, this study could be of interest for researchers that work in other preparations as well. The general conclusions are strongly supported by results that are clearly and elegantly presented.

In this revised submission, the authors addressed all my questions. This is very interesting work that could be of interest for researchers working in other brain areas as well.

Reviewer #2 (Public Review):

This is a very interesting paper with several important findings related to the working mechanism of the cartwheel cells (CWC) in the dorsal cochlear nucleus (DCN). These cells generate spontaneous firing that is inhibited by the activation of α2-adrenergic receptors, which also enhances the synaptic strength in the cells, but the mechanisms underlying the spontaneous firing and the dual regulation by α2-adrenergic receptor activation have remained elusive. By recording these cells with the NALCN sodium-leak channel conditionally knocked, the authors discovered that both the spontaneous firing and the regulation by noradrenaline (NA) require NALCN. Mechanistically, the authors found that activation of the adrenergic receptor or GABAB receptor inhibits NALCN. Interestingly, these receptor activations also suppress the low [Ca2+] "activation" of NALCN currents, suggesting crosstalk between the pathways. The finding of such dominant contribution of the NALCN conductance to the regulation of firing by NA is somewhat surprising considering that NA is known to regulate K+ conductances in many other neurons.

The studies reveal the molecular mechanisms underlying well known regulations of the neuronal processes in the auditory pathway. The results will be important to the understanding of auditory information processing in particular, and, more generally, to the understanding of the regulation of inhibitory neurons and ion channels. The results are convincing and are clearly presented.

In this revision, the authors have satisfactorily addressed all my previous comments.

Reviewer #3 (Public Review):

The study by Ngodup and colleagues describes the contribution of sodium leak NALCN conductance on the effects of noradrenaline on cartwheel interneurons of the DCN. The manuscript is very well-written and the experiments are well-controlled. The scope of the study is of high biological relevance and recapitulates a primary finding of the Khaliq lab (Philippart et al., eLife, 2018) in ventral midbrain dopamine neurons, that Gi/o-coupled receptors inhibit NALCN current to reduce neuronal excitability. Together these studies provide unequivocable evidence for NALCN as a downstream target of these receptors.

In re-review of this study, the authors have addressed the concerns sufficiently. This is a very nice study.

Author Response

The following is the authors' response to the original reviews.

> ***eLife assessment***
>
> *This paper reports the fundamental discovery of adrenergic modulation of spontaneous firing through the inhibition of the Na+ leak channel NALCN in cartwheel cells in the dorsal cochlear nucleus. This study provides unequivocal evidence that the activation of alpha-2 adrenergic or GABA-B receptors inhibit NALCN currents to reduce neuronal excitability. The evidence supporting the conclusions is compelling, the electrophysiological data is high quality and the experimental design is rigorous.*
>
> ***Public Reviews:***
>
> ***Reviewer #1 (Public Review):***
>
> *This study uses electrophysiological techniques in vitro to address the role of the Na+ leak channel NALCN in various physiological functions in cartwheel interneurons of the dorsal cochlear nucleus. Comparing wild type and glycinergic neuron-specific knockout mice for NALCN, the authors show that these channels 1) are required for spontaneous firing, 2) are modulated by noradrenaline (NA, via alpha2 receptors) and GABA (through GABAB receptors), 3) how the modulation by NA enhances IPSCs in these neurons.*
>
> *This work builds on previous results from the Trussell's lab in terms of the physiology of cartwheel cells, and from other labs in terms of the role of NALCN channels, that have been characterized in more and more brain areas somewhat recently; for this reason, this study could be of interest for researchers that work in other preparations as well. The general conclusions are strongly supported by results that are clearly and elegantly presented.*
>
> *I have a few comments that, in my opinion, might help clarify some aspects of the manuscript.*
>
> 1. *It is mentioned throughout the manuscript, including the abstract, that the results suggest a closed apposition of NALCN channels and alpha2 and GABAB receptors. From what I understand, this conclusion comes from the fact that GABAB receptors activate GIRK channels through a membrane-delimited mechanism. Is it possible that these receptors converge on other effectors, for example adenylate cyclase (see https://www.ncbi.nlm.nih.gov/pmc/articles/PMC6374141/).*

We have now tested the role of adenylyl cyclase modulation in the control of NALCN, by saturating the cells with a cAMP analogue 8-Br-cAMP and found no effect on the NA response.

These data are included in the paper. While further experiments are necessary, these results argue in favor of a direct gating by G-proteins.

> 1. *In Figure 2G, the neurons from NALCN KO mice appear to reach a significantly higher frequency than those from WT (figure 2E, 110 vs. 70 spikes/s). Was this higher frequency a feature of all experiments? The results mention a rundown of peak firing rate due to whole-cell dialysis, but, from what I understand, the control conditions should be similar for all experiments.*

The peak firing rates in control solutions for WT and KO CWC are not statistically different.

> 1. *Also in Figure 2, the firing patterns for neurons from WT and NALCN KO mice appear to be quite different, with spikes appearing to be generated during the hyperpolarization of the bursts in the second half of the current step for WT neurons but always during the depolarization in KO neurons. Was this always the case? If so, could NALCN channels be involved in this type of firing? Along these lines, it would be interesting to show an example of a firing pattern of neurons from WT mice in the presence of NA, which inhibits NALCN channels.*

The specific pattern of spikes in CWC is quite variable from trial-to-trial or cell-to-cell, as it is dependent on multiple CaV and calcium dependent K channels subtypes, and is not dependent on the genotypes used here. The primary effects observed in the KO are in background firing and sensitivity to NA, both reflected alterations in rheobase. The firing pattern example requested was shown in the raster plot of fig 2B2.

> 1. *It might be interesting to discuss how the hyperpolarization induced by the activation of GIRK channels and inhibition of NALCN channels could have different consequences due to their opposite effect on the input resistance.*

We considered this as a point of discussion, but decided that making sense of it would depend on assumptions about the location of the channels (dendritic vs somatic, distance to AIS) that we do not have data for. For example, a dendritic increase in resistance through NALCN block, leading to a hyperpolarization of the soma, might have actions similar to a somatic hyperpolarizing conductance increase by GIRK, as far as the voltage at the AIS is concerned.

> ***Reviewer #2 (Public Review):***
>
> *This is a very interesting paper with several important findings related to the working mechanism of the cartwheel cells (CWC) in the dorsal cochlear nucleus (DCN). These cells generate spontaneous firing that is inhibited by the activation of α2-adrenergic receptors, which also enhances the synaptic strength in the cells, but the mechanisms underlying the spontaneous firing and the dual regulation by α2-adrenergic receptor activation have remained elusive. By recording these cells with the NALCN sodium-leak channel conditionally knocked, the authors discovered that both the spontaneous firing and the regulation by noradrenaline (NA) require NALCN. Mechanistically, the authors found that activation of the adrenergic receptor or GABAB receptor inhibits NALCN. Interestingly, these receptor activations also suppress the low [Ca2+] "activation" of NALCN currents, suggesting crosstalk between the pathways. The finding of such dominant contribution of the NALCN conductance to the regulation of firing by NA is somewhat surprising considering that NA is known to regulate K+ conductances in many other neurons.*
>
> *The studies reveal the molecular mechanisms underlying well known regulations of the neuronal processes in the auditory pathway. The results will be important to the*

> *understanding of auditory information processing in particular, and, more generally, to the understanding of the regulation of inhibitory neurons and ion channels. The results are convincing and are clearly presented.*
>
> ***Reviewer #3 (Public Review):***
>
> *The study by Ngodup and colleagues describes the contribution of sodium leak NALCN conductance on the effects of noradrenaline on cartwheel interneurons of the DCN. The manuscript is very well-written and the experiments are well-controlled. The scope of the study is of high biological relevance and recapitulates a primary finding of the Khaliq lab (Philippart et al., eLife, 2018) in ventral midbrain dopamine neurons, that Gi/o-coupled receptors inhibit NALCN current to reduce neuronal excitability. Together these studies provide unequivocable evidence for NALCN as a downstream target of these receptors. There are no major concerns. I have only minor suggestions:*
>
> *Minor*
>
> 1. *As introduced in the introduction, NALCN is inhibited by extracellular calcium which has led to some discourse of the relevance of NALCN when recorded in 0.1 mM calcium. A strength of this study is the effect of NA on NALCN is recorded in physiological levels of calcium (1.2 mM). I suggest including the concentration of extracellular calcium in the aCSF in the Results section instead of relying on the reader to look to the Methods.*

Done.

> 1. *It would be interesting to include the basal membrane properties of the KO compared to wildtype, including membrane resistance and resting membrane potential. From the example recording in Figure 2, one might think that the KOs have lower membrane resistance, so it is interesting that the 2 mV hyperpolarization produced similar effects on rheobase. In addition, from the example in Figure 2G, it appears that NA has an effect on firing frequency with large current injection in the KO. Is this true in grouped data and if so, is there any speculation into how this occurs?*

We have included in the text a comparison of the input resistance in WT and KO. These were not different. This should not be too surprising given the wide range of values between animals, and the necessity to compare populations. Measurements of resting potential are complicated by the fact that CWC are normally spontaneously active. As was discussed in the text, peak firing frequency declined with time during recording in both control and KO, necessitating normalization as shown in Fig 2E-H.

> 1. *Please expand on the rationale for why GABAB and alpha2 must be physically close to NALCN. To my knowledge, the mechanism by which these receptors inhibit NALCN is not known. Must it be membrane-delimited?*

Given the known membrane delimited modulation of GIRK by GABAB, and that alpha2 and GABAB receptors appear to share the same population of NALCN channels, and that alpha2 receptors do not appear to target GIRK channels, we felt the simplest explanation would be coupling through G-proteins, with spatial segregation of different receptor/channel pools providing the means for separating GIRK and NALCN effects. Given that the alpha2 receptor is a Gi/o GPCR, we have now included in the revision new experiments using 8-Br-cAMP, as discussed above. These showed no effect on the NA response, consistent with a direct effect membrane delimited of G-proteins. We acknowledge however that further experiments are warranted.

> ***Reviewer #1 (Recommendations For The Authors):***
>
> *1. I suggest labeling the voltage traces in Figure 2 with WT and KO for easier comprehension; in addition, I suggest adding the average data to the plots in Figure 2, as in Figure 2-supplementary Figure 1 panel F.*

We have added the figure labels as requested. We chose not to add the average data as we noticed that averaging the full FI plots led to a smearing of the curves and a distortion in the apparent rheobase. Thus, we instead measured the rheobase for individual cells and report their average.

> *1. For readers that are not familiar with the field, more details should be given about the electrical stimulation to evoke IPSCs in cartwheel cells, and what they represent.*

Done.

> *1. The methods should mention if and how the concentrations of divalents were adjusted in the experiments with 0.1 extracellular Ca2+*

Done.

> ***Reviewer #2 (Recommendations For The Authors):***
>
> *I only have several minor comments.*
>
> *1. The total lack of spontaneous firing in CWCs in the NALCN KO (Fig. 1) is interesting and provides an opportunity to probe the in vivo function of such spontaneous firing. Besides being a little smaller, do the mutant mice have any sign of abnormality in sound signal processing?*

Figure 1 – Figure supplement 1 showed that there are no effects on auditory brainstem responses in the KO.

> *1. Figs. 3&4 (and several other figures with voltage-clamp recordings), a line indicating zero current level would be useful.*

Done

> *1. page 7, "Outward current generated by suppression of NALCN": it might be better to state as "Outward response generated by suppression of NALCN", as the authors correctly pointed out that the NA-induced apparently outward current response is largely a result of an inhibition of NALCN-mediated inward Na+ current. One way to clarify this might be to record at the Nernst potential of K+ to isolate the contribution of Na+ currents (unclear if K+- or Cs+-based pipette was used in the experiment in Fig 3).*

Text has been modified.

> *1. Figs. 5,6&7: do the dashed lines indicate initial current level or zero current level?*

Initial current. See legends.

1. *The labeling of some of the bar graphs can be made more clear. For example, in Fig. 2K, the right two columns should be labeled as WT as well. Fig. 3C & Fig. 4C, the left two columns should be labeled as WT and the right two as KO.*

Added labels to Fig 2 as requested.

1. *Figs. 5-7: The suppression of low extracellular [Ca2+]-induced NALCN-dependent current by NA and baclofen is very interesting. As the tonic inhibition of NALCN by extracellular Ca2+ is likely through a Ca2+-sensing GPCR (CaSR) and G-proteins (lowering [Ca2+] releases the inhibition and generates inward current) (Lu et al. 2010), the action of NA and baclofen may all converge onto the same G-protein dependent pathway of the Ca2+-sensing receptor. I'd include this in the discussion to provide a potential mechanistic explanation of the interesting observation.*

This is indeed an interesting idea. We prefer not to discuss here, as 1) the source of Ca2+ sensitivity of the channel seems to be controversial (Chua et al 2020), and 2) the effect of Ca2+ reduction is enormously slower than the effect of the modulators (Fig 5-7), implying distinct mechanisms.

Reviewer #3 (Recommendations For The Authors):

Typos/general comments

1. *Figure 2 would be easier to comprehend with WT and KO labels as in the other figures. Done*

1. *Page 11, size of the IPSCs in NA is missing the minus sign.*

Corrected.

1. *Is the y-axis correct on Figure 8B? This looks like it is doubling the size of the IPSC.*

Thank you for catching this mistake. The formula used to calculate % change was in error. We have corrected all the data analysis in the figure, which fortunately did not change the conclusion. Regarding the axis, note that the measurement was % change, not ratio of drug vs control.